Chapter 16

Non-compartmental Analysis

Johan Gabrielsson and Daniel Weiner

Abstract

When analyzing pharmacokinetic data, one generally employs either model fitting using nonlinear regression analysis or non-compartmental analysis techniques (NCA). The method one actually employs depends on what is required from the analysis. If the primary requirement is to determine the degree of exposure following administration of a drug (such as AUC), and perhaps the drug's associated pharmacokinetic parameters, such as clearance, elimination half-life, T_{max}, C_{max}, etc., then NCA is generally the preferred methodology to use in that it requires fewer assumptions than model-based approaches. In this chapter we cover NCA methodologies, which utilize application of the trapezoidal rule for measurements of the area under the plasma concentration–time curve. This method, which generally applies to first-order (linear) models (although it is often used to assess if a drug's pharmacokinetics are nonlinear when several dose levels are administered), has few underlying assumptions and can readily be automated.

In addition, because sparse data sampling methods are often utilized in toxicokinetic (TK) studies, NCA methodology appropriate for sparse data is also discussed.

Key words: Non-compartmental, NCA, AUC, Toxicokinetic, TK, λ_z

1. Non-compartmental Analysis

1.1. Non-compartmental Versus Regression Analysis

Most current approaches to characterize a drug's kinetics involve non-compartmental analysis, denoted *NCA*, and nonlinear regression analysis (1). The advantages of the regression analysis approach are the disadvantages of the non-compartmental approach and vice versa. *NCA* does not require the assumption of a specific compartmental model for either drug or metabolite. The method used involves application of the trapezoidal rule for measurements of the area under a plasma concentration–time curve. This method, which applies to first-order (linear) models, is rather assumption free and can readily be automated. Figure 1 gives a schematic picture of the *NCA* and nonlinear regression approaches. As can be seen, *NCA* deals with sums of areas whereas regression

Brad Reisfeld and Arthur N. Mayeno (eds.), *Computational Toxicology: Volume I*, Methods in Molecular Biology, vol. 929,
DOI 10.1007/978-1-62703-050-2_16,

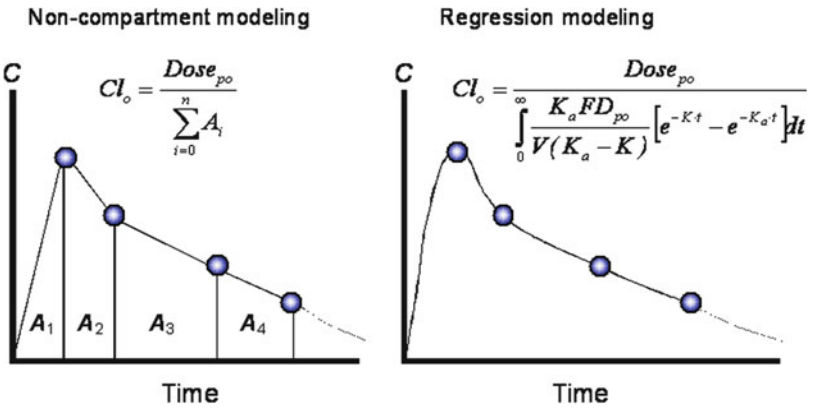

Fig. 1. Comparison of NCA (*left*) and nonlinear regression modeling (*right*). K_a, K, and V in the *right-hand panel* indicate the model parameters to be estimated by regressing the model to data.

modeling uses a function with regression parameters. Both methods are applied for the characterization of the kinetics of a compound.

The time course of drug concentration in plasma can usually be regarded as a statistical distribution curve. The area under a plot of the plasma concentration versus time curve is referred to as the area under the zero moment curve AUC, and the area under the product of the concentration and time versus time curve is then called the area under the first moment curve $AUMC$. Only the areas of the zero and first moments are generally used in pharmacokinetic analysis, because the higher moments are prone to an unacceptable level of computational error.

This section focuses on *NCA* with regard to computational methods, strategies for estimation of λ_z, pertinent pharmacokinetic estimates, issues related to steady state, and how to tackle situations where $t_{1/2}$ is much less than input time.

1.2. Computational Methods: Linear Trapezoidal Rule

The areas can either be calculated by means of the *linear trapezoidal rule* or by the *log-linear trapezoidal rule*. The total area is then measured by summing the incremental area of each trapezoid (Fig. 2).

The magnitude of the error associated with the estimated area depends on the width of the trapezoid and the curvature of the *true* profile. This is due to the fact that the linear trapezoidal rule overestimates the area during the descending phase assuming elimination is *first-order*, and underestimates the area during the ascending part of the curve (Fig. 3). This over/underestimation error will be more pronounced if the sampling interval Δt is large in relation to the half-life.

Using the linear trapezoidal method for calculation of the area under the zero moment curve AUC from 0 to time t_n, we have

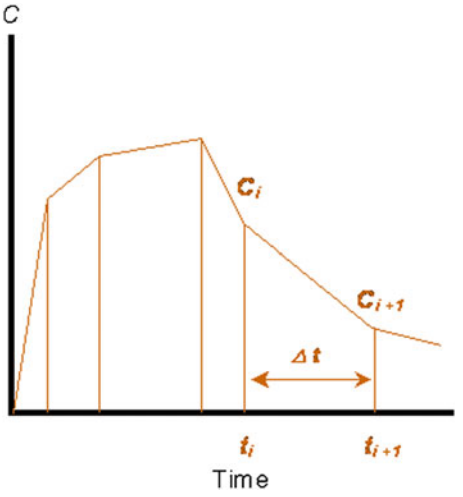

Fig. 2. Graphical presentation of the linear trapezoidal rule. $AUC_{t_i - t_{(i+1)}}$ is the area between t_i and t_{i+1}. C_i and C_{i+1} are the corresponding plasma concentrations, and Δt is the time interval. Note that Δt may differ for different trapeziums.

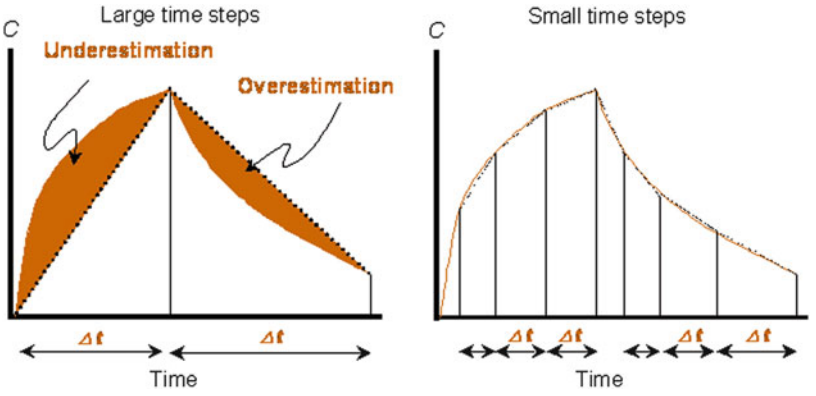

Fig. 3. Concentration versus time during and after a constant rate infusion. The *shaded area* represents underestimation of the area during ascending concentrations and overestimation of the area during descending concentrations. By decreasing the time step (Δt) between observations, this under- or overestimation of the area is minimized.

$$AUC_0^{t_{\text{last}}} = \sum_{i=1}^{n} \frac{C_i + C_{i+1}}{2} \cdot \Delta t, \tag{1}$$

where $\Delta t = t_{i+1} - t_i$ and t_{last} denotes the time of the last measurable concentration. Unless one has sampled long enough in time so that concentrations are negligible, the AUC as defined above will underestimate the *true* AUC. Therefore it may be necessary to extrapolate the curve out to t equal to infinity (∞). The extrapolated area under the zero moment curve from the last sampling time to infinity $AUC_{t_{\text{last}}-\infty}$ is calculated as

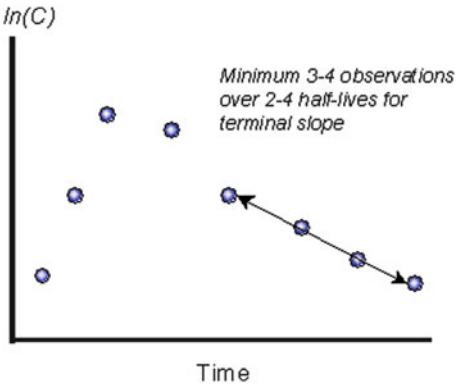

Fig. 4. Semilog plot demonstrating the estimation of λ_z. The terminal data points are fit by log-linear regression to estimate the slope.

$$AUC_{t_{\text{last}}}^{\infty} = \int_{t_{\text{last}}}^{\infty} C_{\text{last}} \cdot e^{-\lambda_z (t - t_{\text{last}})} dt = C_{\text{last}} \left[\frac{e^{-\lambda_z (t - t_{\text{last}})}}{-\lambda_z} \right]_{t_{\text{last}}}^{\infty}$$
$$= C_{\text{last}} \left[0 - \frac{1}{-\lambda_z} \right] = \frac{C_{\text{last}}}{\lambda_z}, \quad (2)$$

where C_{last} and λ_z are the last measurable nonzero plasma concentration and the terminal slope on a $\log_e$ scale, respectively. One may also use the predicted concentration at t_{last} if the observed concentration deviates from the terminal regression line (Fig. 4).

The λ_z parameter is graphically obtained from the terminal slope of the semilogarithmic concentration–time curve as shown in Fig. 4, with a minimum of 3–4 observations being required for accurate estimation. The Y axis $\ln(C)$ denotes the natural logarithm ($\log_e$) of the plasma concentration C.

The linear trapezoidal method for calculation of the area under the first moment curve $AUMC$ from 0 to time t_{last} is obtained from

$$AUMC_0^{t_{\text{last}}} = \sum_{i=1}^{n} \frac{t_i \cdot C_i + t_{i+1} \cdot C_{i+1}}{2} \cdot \Delta t. \quad (3)$$

Remembering that $\int x \cdot e^{-a \cdot x} dx = -\frac{x \cdot e^{-a \cdot x}}{a} - \frac{e^{-a \cdot x}}{a^2}$, the corresponding area under the first moment curve from time t_{last} to infinity $AUMC_{t_{\text{last}}\text{-}\infty}$ is computed as

$$AUMC_{t_{\text{last}}}^{\infty} = \int_{t_{\text{last}}}^{\infty} t \cdot C dt = \int_{t_{\text{last}}}^{\infty} t \cdot C_{\text{last}} e^{-\lambda_z (t - t_{\text{last}})} dt$$
$$= C_{\text{last}} \cdot e^{\lambda_z t_{\text{last}}} \left[\frac{t \cdot e^{-\lambda_z t_{\text{last}}}}{-\lambda_z} + \frac{e^{-\lambda_z t_{\text{last}}}}{-\lambda_z^2} \right]_{t_{\text{last}}}^{\infty}$$
$$= \frac{C_{\text{last}} \cdot t_{\text{last}}}{\lambda_z} + \frac{C_{\text{last}}}{\lambda_z^2}. \quad (4)$$

1.3. Computational Methods: Log-Linear Trapezoidal Rule

An alternative procedure that has been proposed is the log-linear trapezoidal rule. The underlying assumption is that the plasma concentrations decline mono-exponentially between two measured concentrations. However, this method applies only for descending data and fails when $C_i = 0$ or $C_{i+1} = C_i$. In these instances one would revert to the linear trapezoidal rule. The principal difference between the linear and the log-linear trapezoidal method is demonstrated in Fig. 5.

Remember that when the concentrations decline exponentially

$$C_{i+1} = C_i \cdot \mathrm{e}^{-K(t_{i+1}-t_i)} = C_i \cdot \mathrm{e}^{-K\Delta t}, \tag{5}$$

where $t_{i+1} - t_i$ is the time step Δt between two observations and K is the elimination rate constant for a one-compartment system. Otherwise, λ_z should be used as the slope. The above expression when rearranged gives the elimination rate constant K:

$$K = \frac{\ln(C_i/C_{i+1})}{\Delta t}. \tag{6}$$

The AUC within the time interval Δt is the difference between the concentrations divided by the slope K:

$$AUC_i^{i+1} = \frac{C_i - C_{i+1}}{K} = \frac{C_i - C_{i+1}}{\ln(C_i/C_{i+1})} \cdot \Delta t. \tag{7}$$

Using the log-linear trapezoidal method from time zero to t_n

$$AUC_0^{t_n} = \sum_{i=1}^{n} \frac{C_i - C_{i+1}}{\ln(C_i/C_{i+1})} \cdot \Delta t, \tag{8}$$

while the corresponding equation for $AUMC$ from time zero to t_n with this method yields

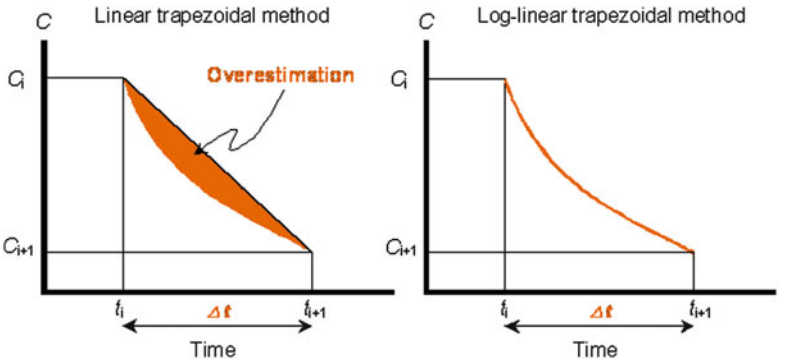

Fig. 5. The principal difference between the linear (*left*) and the log-linear (*right*) trapezoidal methods. The *shaded region* represents the over-predicted area with the linear trapezoidal rule. Note that the log-linear approximation is only true if the decay is truly mono-exponential between t_i and t_{i+1}.

$$AUMC_0^{t_n} = \sum_{i=1}^{n} \frac{t_i \cdot C_i - t_{i+1} \cdot C_{i+1}}{\ln(C_i/C_{i+1})} \cdot \Delta t - \frac{C_{i+1} - C_i}{[\ln(C_i/C_{i+1})]^2} \cdot \Delta t^2. \tag{9}$$

The extrapolated area under the zero moment curve from the last sampling time to infinity $AUC_{t_{last}\text{-}\infty}$ is calculated as

$$AUC_{t_{last}}^{\infty} = \frac{C_{last}}{\lambda_z}, \tag{10}$$

where C_{last} and λ_z are as defined earlier. The corresponding area under the first moment curve from time zero to infinity $AUMC_{t_{last}\text{-}\infty}$ is

$$AUMC_{t_{last}}^{\infty} = \frac{C_{last} \cdot t_{last}}{\lambda_z} + \frac{C_{last}}{\lambda_z^2}. \tag{11}$$

As previously pointed out, the linear trapezoidal method gives approximate estimates of AUC during both the ascending and descending parts of the concentration–time curve, although the bias is usually negligible for the upswing. The log-linear trapezoidal method may also give somewhat biased results, though to a lesser extent. Some people argue that the log-linear trapezoidal method may therefore be preferable for drugs with long half-lives relative to the sampling interval. From a practical point of view this still needs to be proven. However, our own experience is that the difference between the two methods is negligible as long as a reasonable sampling design has been used. We generally use a mixture of the two methods, which means that the linear trapezoidal method is applied for increasing and equal concentrations, e.g., at the peak or a plateau, and the log-linear trapezoidal method for decreasing concentrations. This is demonstrated in Fig. 6.

Note that *NCA* is often used in crossover studies comparing two formulations and 12–36 subjects. Thus, since the error associated

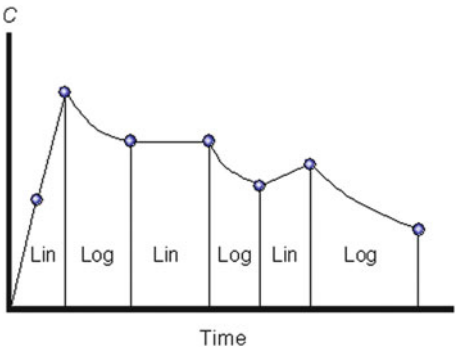

Fig. 6. NCA using a combination of the linear and log-linear trapezoidal methods. The linear method is used for consecutively increasing or consecutively equal concentrations. The log-linear method is used for decreasing concentrations.

with an individual patient's AUC is generally small, the (average) error associated with the average AUC for a formulation will generally be negligible, regardless of the method used. The choice of method is thus up to the discretion of the modeler, as long as one can explain why a particular method provides a more accurate estimate of AUC.

The linear trapezoidal method will work excellently in situations of zero-order kinetics since plasma concentrations decline linearly with time. Hence, even large sampling intervals will be acceptable. The log-linear trapezoidal rule may in some instances be more optimal within the first-order concentration range. The linear method will then overpredict the areas particularly when half-life is short relative to the sampling interval.

Direct integration of the function for the drug's kinetics in plasma is discussed under the introductory section on mono- and multi-exponential models and will therefore not be further elaborated here.

1.4. Strategies for Estimation of λ_z

When estimating λ_z, we recommend that data from each individual are first plotted in a semilog diagram. Ideally, to obtain a reliable estimate of the terminal slope, 3–4 half-lives would need to have elapsed. However, sometimes this is not possible. A minimum requirement is then to have 3–4 observations for the terminal slope (Fig. 7). By means of log-linear regression of those observations, the estimate of λ_z is obtained. This is then used for calculation of the extrapolated area as shown below:

$$AUC_{t_{\text{last}}}^{\infty}(\text{observed}) = \frac{C_{\text{last}}}{\lambda_z} \tag{12}$$

or

$$AUC_{t_{\text{last}}}^{\infty}(\text{predicted}) = \frac{\hat{C}_{\text{last}}}{\lambda_z}. \tag{13}$$

In Fig. 8 the last observed concentration C_{obs} deviates somewhat from the regression line. The extrapolated area, if based on

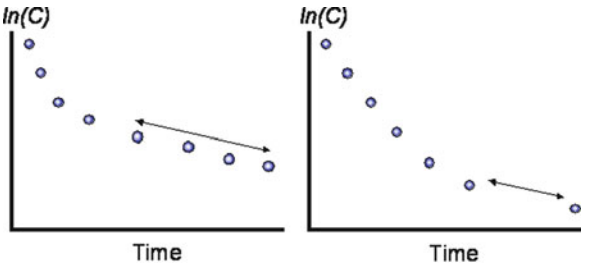

Fig. 7. The ideal situation (*left*) for estimation of the terminal slope λ_z. Another and perhaps more commonly encountered situation (*right*) is where one only has an indication of an additional slope.

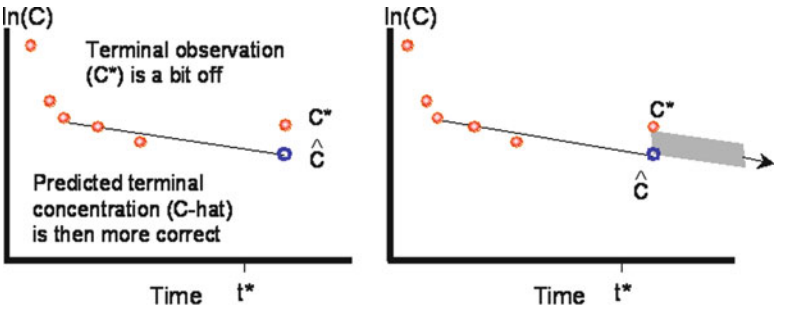

Fig. 8. Impact on the extrapolated area of using observed terminal concentration versus predicted concentration. The *shaded area* from t_{last} to infinity symbolizes the overestimation that would result. Note that if the observed terminal concentration lies below the predicted terminal concentration, then the extrapolated area would be underestimated. The *open circle* is the predicted concentration at t_{last}. The last observation is not included in the regression.

C_{obs}, would be disproportionately large as compared to the area based on the predicted concentration.

The total area is obtained by summing the individual areas obtained by means of the trapezoidal rule to the last time (t_{last}), and adding the extrapolated area according to

$$AUC_{total} = AUC_0^{\infty} = AUC_0^{t_{last}} + AUC_{t_{last}}^{\infty}. \quad (14)$$

The fraction of AUC_{extr} to $AUC_{0\text{-}\infty}$ is calculated as

$$\%\,\text{extrapolated area} = \frac{AUC_{t_{last}}^{\infty}}{AUC_0^{\infty}} \cdot 100. \quad (15)$$

The extrapolated area should ideally be as small as possible in comparison to the total area. We believe that $AUC_{t_{last}\text{-}\infty}$ should not exceed 20–25% of AUC_{total}, unless it is only used as a preliminary estimate for further study refinement.

1.5. Pertinent Pharmacokinetic Estimates

Moment analysis has been widely used in recent years as a non-compartmental approach to the estimation of clearance *Cl*, mean residence time *MRT*, steady-state volume of distribution V_{ss}, and volume of distribution during the terminal phase V_z (also called $V_{d\beta}$ for a bi-exponential system). A general treatment for the aforementioned parameters has been presented, which includes the possibility of input/exit from any compartment in a mammillary model (2, 3). This approach also defines *exit site-dependent* and *exit site-independent* parameters. We will, however, assume in the following examples that input/output occurs to the central compartment. Assuming a simple case with a one-compartment bolus system, the shape of the *concentration–time* and *t·concentration–time* profiles will take the form depicted in Fig. 9.

The extrapolated area from the last sample at t_{last} to infinity is in this case small. However, the corresponding area under the first

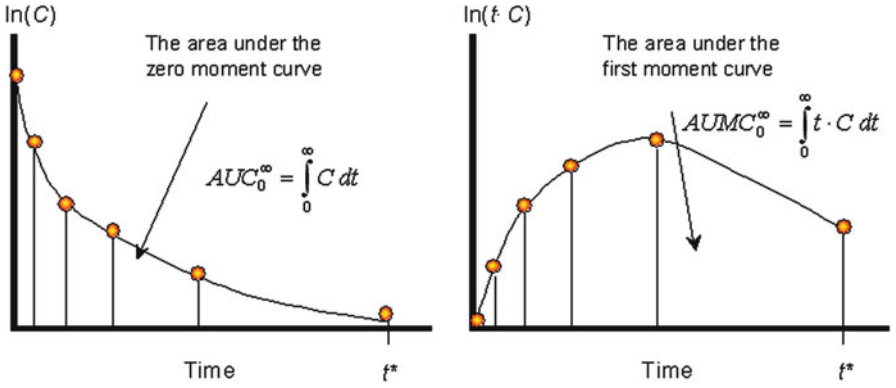

Fig. 9. Comparison of shape of area under the zero moment curve AUC and area under the first moment ($t \cdot C$) curve AUMC. The latter area contains usually an extensive extrapolated area as compared to AUC.

moment curve has an altogether different shape. Clearly, the extrapolated area from last sampling point to infinity will generally contribute to a much larger extent under the first moment curve as compared to the area under the zero moment curve.

Pharmacokinetics has moved almost completely from parameterizing elimination in terms of rate constants, with the more physiologically relevant use of clearance now being widely recognized. To put even more focus on clearance, Holford suggested that AUC no longer be used as a pharmacokinetic parameter. Clearance Cl or clearance over bioavailability Cl/F also denoted that Cl_0 is easily computed from AUC and dose, and Cl and CL/F can immediately be interpreted in a physiological context. On the other hand, AUC can be viewed as a parameter that confounds clearance and dose, and that has no intrinsic merit. While we agree with those ideas, AUC is still useful as a measure of exposure in toxicological studies and when dose is unknown.

Clearance is calculated from the dose and the area under the zero moment curve:

$$Cl = \frac{D_{\mathrm{iv}}}{AUC_0^\infty}. \tag{16}$$

Oral clearance Cl_0 or Cl/F is calculated from the oral dose and the area under the zero moment curve:

$$Cl_0 = \frac{Cl}{F} = \frac{D_{\mathrm{po}}}{AUC_0^\infty}. \tag{17}$$

Using the areas obtained from systemic, e.g., intravenous and extravascular, e.g., oral, dosing, the bioavailability F is calculated, after dose-normalization, according to

$$F = \frac{AUC_{\mathrm{ev}}}{AUC_{\mathrm{iv}}} \cdot \frac{D_{\mathrm{iv}}}{D_{\mathrm{ev}}}, \tag{18}$$

where AUC_{ev} and AUC_{iv} denote area under the extravascular and intravenous concentration–time profiles, respectively. D_{ev} and D_{ev} are the respective extravascular and intravenous doses.

If the drug is given at a constant rate over a period of T_{inf}, then one also needs to adjust *MRT* for the infusion time by means of subtracting $T_{inf}/2$ (infusion time/2) as follows:

$$MRT = \frac{AUMC_0^\infty}{AUC_0^\infty} - \frac{T_{inf}}{2}. \tag{19}$$

$T_{inf}/2$ originates from the average time a molecule stays in the infusion set (e.g., syringe, catheter, line). Half of the dose is infused when the piston has traveled half of the intended distance. $T_{inf}/2$ is the mean input time, *MIT*. Similarly for *first-order* input,

$$MRT = \frac{AUMC_0^\infty}{AUC_0^\infty} - \frac{1}{K_a}. \tag{20}$$

Remember that K_a is the apparent *first-order* absorption rate constant derived from plasma data. This parameter may also contain processes parallel to the true absorption step of drug in the gastrointestinal tract, e.g., chemical degradation (k_d). Consequently, the mean absorption time, *MAT*, is the sum of several processes including absorption and chemical degradation:

$$MAT = \frac{1}{K_{a(apparent)}} = \frac{1}{K_{a(true)} + k_d}. \tag{21}$$

The *MRT* of the central compartment *MRT*(1) is the sum of the inverse of the initial α and terminal β slopes corrected for the inverse of the sum of the exit rate constants from the peripheral compartment:

$$MRT_{iv}(1) = \frac{1}{\alpha} + \frac{1}{\beta} - \frac{1}{E_2}. \tag{22}$$

Assuming that there is only one exit rate constant from the peripheral compartment, which then is k_{21}, the MRT_{iv} is

$$MRT_{iv} = \frac{1}{\alpha} + \frac{1}{\beta} - \frac{1}{k_{21}}. \tag{23}$$

The observed *MRT* after extravascular dosing becomes

$$\frac{AUMC_{0\,measured}^\infty}{AUC_{0\,measured}^\infty} = MRT + MIT, \tag{24}$$

which is the sum of the true *MRT* and *MIT*. *MIT* can also be obtained from the input function according to Eq. 25 below:

$$MIT = \frac{\int_0^\infty \text{input function} \cdot t\,dt}{\int_0^\infty \text{input function}\,dt} = \frac{\int_0^\infty \text{input function} \cdot t\,dt}{F \cdot \text{Dose}}, \tag{25}$$

provided the input function is known,

$$A_{\text{gut}} = F \cdot D_{\text{po}} \cdot \mathrm{e}^{-K_{\text{a}} \cdot t}, \tag{26}$$

and *MIT* can be derived:

$$MIT = \frac{\int_0^\infty F \cdot D_{\text{po}} \cdot \mathrm{e}^{-K_{\text{a}} \cdot t} \cdot t \, \mathrm{d}t}{\int_0^\infty F \cdot D_{\text{po}} \cdot \mathrm{e}^{-K_{\text{a}} \cdot t} \, \mathrm{d}t} = \frac{F \cdot D_{\text{po}} / K_{\text{a}}^2}{F \cdot D_{\text{po}} / K_{\text{a}}} = \frac{1}{K_{\text{a}}}. \tag{27}$$

The volume of distribution at steady-state V_{ss} is computed as

$$V_{\text{ss}} = MRT \cdot Cl = \frac{AUMC_0^\infty}{AUC_0^\infty} \cdot \frac{D_{\text{iv}}}{AUC_0^\infty} = \frac{D_{\text{iv}} \cdot AUMC_0^\infty}{\left[AUC_0^\infty\right]^2}. \tag{28}$$

The volume of distribution during the terminal phase V_{z} is computed as

$$V_{\text{z}} = \frac{Cl}{\lambda_{\text{z}}} = \frac{D_{\text{iv}}}{AUC_0^\infty} \cdot \frac{1}{\lambda_{\text{z}}}. \tag{29}$$

The corresponding volume for a bi-exponential function is computed as

$$V_{d\beta} = \frac{Cl}{\beta} = \frac{D_{\text{iv}}}{AUC_0^\infty} \cdot \frac{1}{\beta}. \tag{30}$$

The terminal half-life $t_{1/2\text{z}}$ is readily estimated from the slope λ_{z} as

$$t_{1/2\text{z}} = \frac{\ln(2)}{\lambda_{\text{z}}}. \tag{31}$$

The half-life of the initial α-phase is

$$t_{1/2\alpha} = \frac{\ln(2)}{\alpha}. \tag{32}$$

The half-life of the terminal β-phase of a bi-exponential function is

$$t_{1/2\beta} = \frac{\ln(2)}{\beta}. \tag{33}$$

Note that the $t_{1/2\text{z}}$ parameter is referred to as $t_{1/2\beta}$ in a bi-exponential function and simply $t_{1/2}$ in a mono-exponential system.

1.6. NCA Approaches for Sparse Data

In some instances it may not be possible to obtain sufficient samples from each subject so as to completely characterize the plasma concentration–time curve. This may be due to the need to sacrifice the animal to obtain the samples, general concerns over blood loss (such as in human neonates or small rodents), or cost concerns. In these situations it is necessary to pool the data from multiple

subjects to characterize the full time–plasma concentration curve. Generally these approaches are recommended only when the data are being collected from populations that do not exhibit extensive subject-to-subject variation, such as in highly inbred strains of animals.

One such approach is an extension of the NCA analysis for rich data described previously, and enables one to derive an estimated standard error (se) for AUC for sparse data (4–6). This procedure is implemented in Phoenix® WinNonlin®.

Another approach has also been proposed that involves nonlinear mixed effects modeling (also denoted as population modeling). In this instance a structural pk model is specified and fit to the data. This approach has the advantage of incorporating covariates (e.g., age, gender, body weight, etc.). That is, the ability (e.g.) to model changes in clearance as a function of age or body weight. It also has a limitation of possibly not being able to adequately identify the underlying structural model unless the sparse data can be pooled with rich data from some other cohort (7).

1.7. Suggested Reading

For further reading on basic pharmacokinetic principles, we refer the reader to Benet (8), Benet and Galeazzi (9), Gibaldi and Perrier (10), Nakashima and Benet (2, 3), Jusko (11), and Rowland and Tozer (12). Houston (13) and Pang (14) provide excellent texts on metabolite kinetics.

Benet and Galeazzi (9), Watari and Benet (15), and Nakashima and Benet (3) have elaborated on the theory of *NCA*, while Gillespie (16) discussed the pros and cons of *NCA* versus compartmental models.

References

1. Gabrielsson J, Weiner D (2006) Pharmacokinetic and pharmacodynamic data analysis: concepts and applications, 4th edn. Swedish Pharmaceutical Press, Stockholm
2. Nakashima E, Benet LZ (1988) General treatment of mean residence time, clearance and volume parameters in linear mamillary models with elimination from any compartment. J Pharmacokinet Biopharm 16:475
3. Nakashima E, Benet LZ (1989) An integrated approach to pharmacokinetic analysis for linear mammillary systems in which input and exit may occur in/from any compartment. J Pharmacokinet Biopharm 17:673
4. Bailer AJ (1988) Testing for the equality of area under the curve when using destructive measurement techniques. J Pharmacokinet Biopharm 16:303
5. Yeh C (1990) Estimation and significance tests of area under the curve derived from incomplete blood sampling. In: ASA Proceedings of the Biopharmaceutical Section, p 4
6. Nedelman JR, Jia X (1998) An extension of Satterthwaite's approximation applied to pharmacokinetics. J Biopharm Stat 8(2):317
7. Hing JP, Woolfrey SG, Wright PMC (2001) Analysis of toxicokinetic data using NONMEM: impact of quantification limit and replacement strategies for censored data. J Pharmacokinet Pharmacodyn 28(5):465
8. Benet LZ (1972) General treatment of linear mammillary models with elimination from any compartment as used in pharmacokinetics. J Pharm Sci 61:536
9. Benet LZ, Galeazzi RL (1979) Noncompartmental determination of the steady-state volume of distribution. J Pharm Sci 48:1071
10. Gibaldi M, Perrier D (1982) Pharmacokinetics. Revised and expanded, 2nd edn. Marcel Dekker Inc., New York, NY

11. Jusko WJ (1992) Guidelines for collection and analysis of pharmacokinetic data. In: Evans WE, Schentag JJ, Jusko WJ (eds) Applied pharmacokinetics: principles of therapeutic drug monitoring, 3rd edn. Applied Therapeutics, Spokane, WA
12. Rowland M, Tozer T (2010) Clinical pharmacokinetics and pharmacodynamics: concepts and applications, 4th edn. Lippincott Williams & Wilkins, Maryland
13. Houston JB (1994) Kinetics of disposition of xenobiotics and their metabolites. Drug Metab Drug Interact 6:47
14. Pang KS (1985) A review of metabolic kinetics. J Pharmacokinet Biopharm 13(6):633
15. Watari N, Benet LZ (1989) Determination of mean input time, mean residence time, and steady-state volume of distribution with multiple drug inputs. J Pharmacokinet Biopharm 17 (1):593
16. Gillespie WR (1991) Noncompartmental *versus* compartmental modeling in clinical pharmacokinetics. Clin Pharmacokinet 20:253